Development and Testing of a Variable Conductance Thermal Acquisition, Transport, and Switching System

David C. Bugby[1]
ATK Space, Beltsville, Maryland, 20705

Jeffery T. Farmer[2]
NASA Marshall Space Flight Center, Huntsville, Alabama, 35812

and

Charles J. Stouffer[3]
ATK Space, Beltsville, Maryland, 20705

This paper describes the development and testing of a scalable thermal management architecture for instruments, subsystems, or systems that must operate in severe space environments with wide variations in sink temperature. The architecture involves a serial linkage of one or more hot-side variable conductance heat pipes (VCHPs) to one or more cold-side loop heat pipes (LHPs). The VCHPs provide wide area heat acquisition, limited distance thermal transport, modest against gravity pumping, concentrated LHP startup heating, and high switching ratio variable conductance operation. The LHPs provide localized heat acquisition, long distance thermal transport, significant against gravity pumping, and high switching ratio variable conductance operation. The single-VCHP, single-LHP system described herein was developed to maintain thermal control of a small robotic lunar lander throughout the lunar day-night thermal cycle. It is also applicable to other variable heat rejection space missions in severe environments. Operationally, despite a 60-70% gas blocked VCHP condenser during ON testing, the system was still able to provide 2-4 W/K ON conductance, 0.01 W/K OFF conductance, and an end-to-end switching ratio of 200-400. The paper provides a detailed analysis of VCHP condenser performance, which quantified the gas blockage situation. Future multi-VCHP/multi-LHP thermal management system concepts that provide power/transport length scalability are also discussed.

Nomenclature

A	=	radiator area
D	=	diameter
G	=	conductance
h	=	heat transfer coefficient
L	=	transport length
Q	=	heat flow

I. Introduction

SPACECRAFT that must operate reliably in highly variable-temperature environments like the lunar surface require high conductance thermal acquisition/transport when the environment is hot and low conductance thermal isolation when the environment is cold. This paper describes such a thermal switching architecture, originally developed for lunar landers, involving a hot-side variable conductance heat pipe (VCHP) serially linked to a cold-side loop heat pipe (LHP). Power/transport length scalability is possible via multiple such VCHP-LHP units.

[1] Senior Thermal Engineer, Thermal Technology Group, ATK Space ITS, and AIAA Non-Member.
[2] Lead Thermal Engineer of Robotic Lunar Lander Development Project, NASA/MSFC, and AIAA Member.
[3] Program Manager, Program Management Group, ATK Space ITS, and AIAA Non-Member.

A previous analytical study[1] yielded the VCHP-LHP as the preferred thermal switching solution for an extended duration lunar surface science platform. The thermal control challenge involved the Warm Electronics Box (WEB) on International Lunar Network (ILN) anchor node landers (primarily seismographic measurement stations whose basic design is depicted in the Appendix). The WEB had to be maintained: (a) below 323 K with 60-100 W power dissipation during the 15-earth day, 390 K surface, lunar day (note: a special reflector radiator provides a 269 K sink as shown in the Appendix); and (b) above 263 K with minimal power dissipation during the 15-earth day, 100 K surface, lunar night. In that study, 26 thermal switching architectures were ranked based on the driving requirements of control power, lifetime, fewest interfaces, least complexity, autonomy, and landed tilt tolerance. The VCHP-LHP ultimately ranked highest because it was expected that the VCHP and LHP (both extensively flight-proven) could be designed to provide high thermal conductance, high ON/OFF switching ratio, and autonomous operation with low (or zero) control power. Ground test results provided herein will address the validity of those expectations.

II. Requirements

Over the last several years, NASA Marshall Space Flight Center (NASA/MSFC), in a partnership with the Johns Hopkins University Applied Physics Laboratory (JHU/APL), has evaluated several potential robotic lunar surface missions ranging from water and volatiles prospecting in permanently shadowed lunar craters and nearby polar regions to geophysical science investigations covering the entire lunar surface. These investigations formulated and evaluated designs of robotic lunar landers and science platforms that would operate continuously for up to 6 years at equatorial and mid-latitude locations and autonomous rovers intended to traverse between sunlit and shadowed regions and even from crater rims into permanently shadowed craters. Because of the unique thermal environments encountered in these diverse missions, three thermal control operational modes were identified as required elements of the various thermal management options that were considered:

(1) the ability to transport/reject heat efficiently from dissipation sources within the surface asset (e.g. experiment package, rover, or lander) during sunlit periods where nearby lunar surface temperatures may approach 390 K;

(2) the ability to thermally isolate and conserve heat/power during cold, extended shadowed or night operation; and

(3) the ability to reliably switch back and forth between modes (1) and (2) with minimal operational resources.

To emphasize the importance of the second thermal control mode listed above (thermal isolation, heat/power conservation), the power system team estimated that for every watt of electrical power expended during the entire lunar night, at least 5 kg of battery mass was required to reliably provide this energy. This mass penalty propagated throughout the system, thus for minimum mass/cost robotic missions, saving energy at night was a critical need.

As part of a risk reduction activity for the ILN mission, an effort was undertaken to indentify thermal control hardware that could provide these features and to demonstrate and assess those capabilities. This effort in turn led to an analytical study and a hardware test program (described herein). To evaluate the candidate thermal architectures and design/test the thermal hardware, ILN mission requirements were developed for two power options (solar and advanced Stirling radioisotope generator or ASRG) and those requirements were then adjusted as needed to carry out an initial analytical study and subsequent hardware testing. Table 1 lists the ILN mission thermal requirements.

Table 1. ILN Mission Thermal Requirements

Requirement	ILN Solar	ILN ASRG	Analytical Study	Test Program
Min. Electronics Temp.	263 K	263 K	263 K	263 K
Max. Electronics Temp.	323 K	323 K	303-323 K	323 K
Min. Electronics Power	0 W	40 W	0 W	0 W
Max. Electronics Power	66 W	56 W	60 W	95 W
Elec. Power in Transit	72 W	57 W	72 W	117 W
Trip Length	5 days	5 days	5 days	5 days
Mission Duration	6 years	6 years	6 years	6 years
WEB Geometry	0.61 m x1.04 m x 0.36 m	0.55 m x 0.33 m x 0.38 m	0.55 m x 0.33 m x 0.38 m	0.61 m x1.04 m x 0.36 m
WEB-Radiator Distance	0.36 m	0.36 m	0.36 m	0.36 m
Radiator Area	0.323 m^2	0.323 m^2	0.323 m^2	2 x 0.323 m^2
Maximum Tilt	14°	14°	20°	14°
Radiator Emissivity	0.8	0.8	0.8	0.8
Lunar Day Sink*	269 K	269 K	263 K	269 K
Lunar Night Sink	93-96 K	141 K	141 K	96 K
Cruise Sink	168 K	168 K	168 K	168 K
Min. Soil Temperature	100 K	100 K	100 K	100 K
Max. Soil Temperature	390 K	390 K	390 K	390 K

* Relatively cool lunar day sink of 269 K achieved by specially designed radiator that avoids viewing the sun and the hot lunar surface

III. Architectures

A total of 26 different variable heat rejection (thermal switching) architectures were evaluated in the previous analytical study[1] to meet Table 1 requirements. The considered architectures combined 5 basic fluid-based device types (note: mechanical thermal switches were eliminated from consideration due to controllability, reliability, lifetime, and flight heritage limitations) – *VCHP, LHP, capillary pumped loop (CPL), hybrid loop heat pipe (HLHP), and mechanically pumped loop (MPL)* – with 7 device modifications to enhance system performance – *thermoelectric cooler (TEC), flow-obstructing valve (FV), bypass valve (BV), heat exchanger plus subcooler (HX+SC), additional VCHP, multiple-evaporator/condenser (MEC), and multi-pass (MP) system*. After numerically ranking the architectures by giving each a score of 1-4 (in increments of 0.5) in the 6 driving requirement categories of control power, lifetime, fewest interfaces, least complexity, operational autonomy, and landed tilt tolerance and then computing the total score by multiplying the scores in each category, the top six (and their numerical scores) ended up to be: (1) VCHP-LHP (2240); (2) VCHP-VCHP (1120); (3) LHP-HX+SC (672); (4) VCHP (512) ; (5) LHP-BV (480); and (6) VCHP-LHP-MP (448). The remainder of this section will focus on the VCHP-LHP solution by describing: (i) the thermal switching principles of the VCHP and LHP as stand-alone devices; and (ii) the architectural features of combining the two devices into an integrated variable heat rejection architecture.

A. VCHP Variable Conductance

The VCHP is simply a constant conductance heat pipe (CCHP) with modifications for variable conductance operation (thermal switching). A CCHP is a sealed tube with an internal (end-to-end) porous wick charged with a two-phase working fluid. Heat is added over a given length (L_E) at the evaporator end and removed over a given length (L_C) at the condenser end. Between the evaporator and condenser is the adiabatic section of length (L_A). To modify a CCHP into a VCHP, a small amount of noncondensable gas (NCG) is added to the working fluid charge and a (wick-bearing) NCG reservoir is attached to the condenser end of the tube.

Variable conductance with a VCHP is attained by NCG "gas blockage" in the condenser. When heat is added to a VCHP evaporator, NCG is convected to the condenser/NCG reservoir end, and it resides there as an NCG slug. The extent to which the evaporator-facing side of the slug ("NCG front") protrudes into the VCHP defines the point where condensation ceases. The protrusion distance is based on the NCG reservoir temperature, which controls an internal VCHP pressure balance. The NCG partial pressure plus the working fluid partial pressure in the NCG reservoir equals the internal pressure within the VCHP, which is the working fluid saturation pressure at the evaporator temperature. By controlling the temperature of the NCG reservoir, the NCG front location can be varied from: (a) at the condenser-NCG reservoir boundary (fully ON, condenser "unblocked", max conductance); to (b) within the condenser (partially ON, condenser partially "blocked", variable conductance); to (c) within the adiabatic section (nearly OFF, condenser fully "blocked", very low conductance); to (d) just outside the evaporator (fully OFF, condenser fully "blocked", min conductance). Figure 1 depicts the foregoing description of VCHP operation.

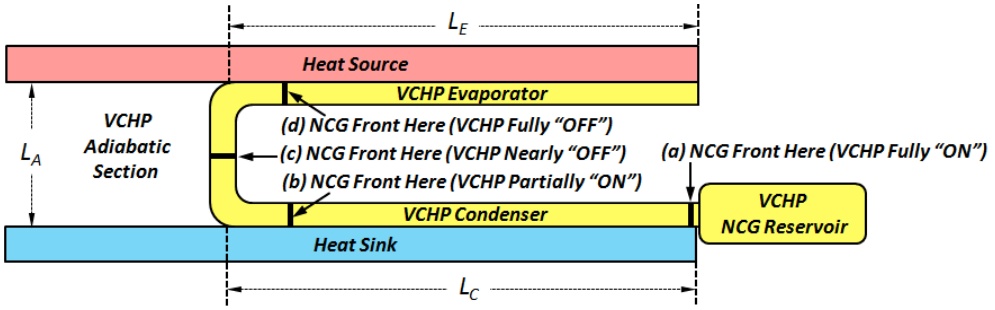

Figure 1. VCHP Variable Conductance by Condenser Noncondensable Gas Blockage

B. LHP Variable Conductance

The LHP is the most prevalent two-phase loop architecture for spacecraft thermal control. The CPL and HLHP are the other two available two-phase loop architectures and the following description applies to them as well. Like heat pipes, LHPs: (i) have no moving parts; (ii) circulate fluid based on the capillary pressure developed in a fine-pore wick; (iii) contain evaporator, condenser, and adiabatic sections; and (iv) are charged with a two-phase working fluid. The adiabatic section of an LHP contains a liquid transport line and a vapor transport line. Unlike heat pipes, the primary (fluid-circulating) wicks in LHPs are confined solely to the evaporator and LHPs also contain a wick-bearing, two-phase fluid reservoir. The LHP condenser and liquid/vapor lines are usually just smooth-walled tubing.

Variable conductance with an LHP is attained by "liquid blockage" in the condenser. Vapor produced at the evaporator flows to the condenser in the vapor line, where it requires a given length (L_O) to condense based on the LHP operating (reservoir) temperature and the radiative sink temperature. The effective radiator area varies in proportion to the fraction $\phi = L_O/L_C$, which represents the "unblocked" condenser fraction. LHP conductance (G) is proportional to ϕ. When circulation ceases, LHP conductance drops nearly to zero, with a remaining small conductive heat leak along the liquid and vapor transport lines, which is similar to the case for a fully-OFF VCHP, wherein heat flows from evaporator to condenser solely by conduction through the VCHP adiabatic section tube wall. Figure 2 illustrates the foregoing description of LHP operation.

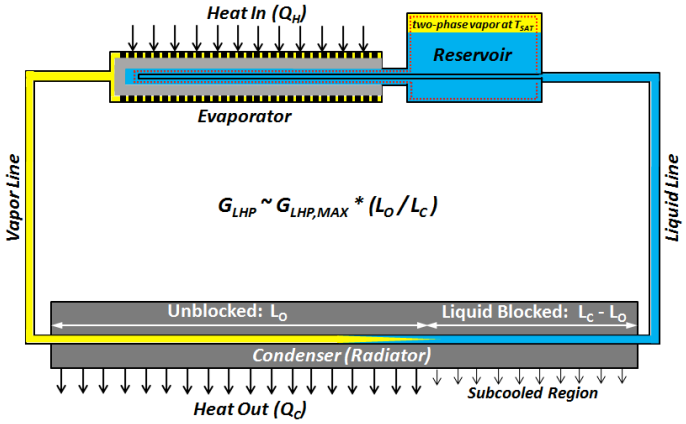

Figure 2. LHP Variable Conductance by Condenser Liquid Blockage

C. VCHP-LHP Architecture

The VCHP-LHP architecture, which is comprised of a serial coupling of one or more hot-side VCHPs to one or more cold-side LHPs (such as the single-VCHP, single-LHP system illustrated in Figure 3), has several advantages for severe-environment NASA missions (such as ILN) requiring variable heat rejection. First, an elongated VCHP evaporator is better at large area, low ΔT heat acquisition than a typical short LHP evaporator. Second, thin-walled tube LHP transport lines and condensers are more weight efficient at low ΔT transport and heat rejection than VCHP adiabatic sections and condensers. Third, because VCHP condenser area grows slowly from a zero area footprint, the high heat flux of VCHP condensation can replace LHP startup heaters. Fourth, passive thermal control, which neither can do easily by themselves, is a possibility with appropriate system architecture. Fifth, the coupled system provides VCHP thermal switching in series with LHP thermal switching, and that combination can provide turn-down ratios of 1000 or more. Lastly, VCHPs are intrinsically freeze-tolerant, which may allow water as a VCHP working fluid and/or operational exposure of the VCHP condenser and reservoir to very cold sinks. The next three sections of this paper will describe the design, testing, and analysis of a single-VCHP, single-LHP demonstration system developed for WEB thermal control on the ILN mission. Following those three sections, the paper will address VCHP-LHP scalability to multi-kW variable heat rejection missions.

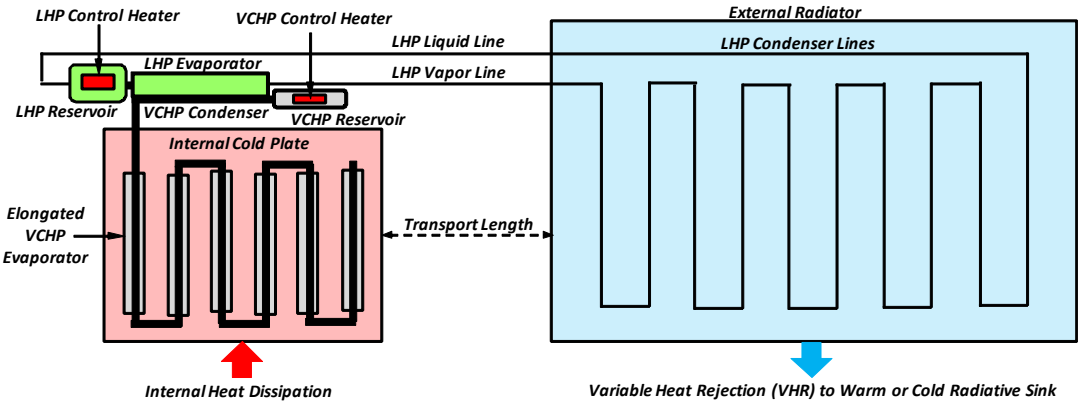

Figure 3. VCHP-LHP Architecture with Single-VCHP and Single-LHP

IV. Design

As previously described herein, the idea for the VCHP-LHP architecture was developed as a result of an analytical study[1] conducted by ATK for NASA/MSFC during the summer of 2009. In that effort, ATK performed a trade study that looked at 26 different variable conductance heat transport systems (VCHTS) and determined that a VCHP-LHP with dual ammonia VCHPs in series with a single propylene LHP would best meet the thermal control system needs of the WEB on ILN anchor node lunar landers. The ILN thermal requirements for this analytical study (as well as the follow-on hardware test program described herein) were previously provided in Table 1.

During the study, a total of 36 different VCHTS requirements were identified. The key system discriminators included: (1) control power (minimize due to 5.5 kg/W mass penalty); (2) lifetime (6 year minimum); (3) vertical integration ability (a measure of how few interfaces the system would require); (4) complexity (the goal was the simplest system possible); (5) autonomous operation (desired, not required); and (6) landed adverse tilt tolerance (operation required with +/- 15º tilts in any direction). It is anticipated that these key system requirements might be modestly applicable to other future NASA missions requiring variable heat rejection technology.

Following the study, a three-step hardware development risk reduction sequence was carried out to meet the test program requirements listed in Table 1. In step 1, a propylene LHP test system with a Teflon primary wick for low power startups was designed, built, and tested. In step 2, an ammonia VCHP stand-alone test unit that could be integrated directly into the LHP test system was built and tested. In step 3, the VCHP was integrated into the LHP test system and the coupled VCHP-LHP test system was tested. Test results from the VCHP-LHP are provided in the following section. Overall, the VCHP-LHP test unit was able to meet WEB thermal control requirements during thermal vacuum testing. The remainder of this section addresses test hardware design.

A. LHP Test System

The first step in the risk reduction sequence described above was the design and testing of a propylene LHP test system. As illustrated in Figure 4, this test system was comprised of the following elements: ***(a) LHP evaporator*** (aluminum body, Teflon wick, 0.3 m length, 0.02 m outer diameter, 0.05 m flange width); ***(b) LHP reservoir*** (stainless steel body); ***(c) propylene working fluid*** to prevent freezing with a 100 K sink; ***(d) horizontal radiator*** for capillary-pumped operation (two-sided, 0.16 m^2 each side, aluminum, black paint); ***(e) vertical radiator*** for gravity-pumped operation (two-sided, 0.16 m^2 each side, aluminum, black paint); ***(f) liquid/vapor lines*** (1 m length, stainless steel); ***(g) co-located flow regulator (CLFR)*** to isolate a cold active radiator from a warm inactive radiator; ***(h) WEB simulator plate*** (aluminum, black paint, isolated with small radiative coupling to LHP reservoir); and ***(i) mounting frame*** that provides for two test configurations as shown in Figure 4. Testing of the LHP test system was largely successful; however, a few operational anomalies were encountered when the system was tested with rapid variations (in excess of expected flight variations) in radiator sink temperature and instrument power. The root cause of these anomalies was that the CLFR wick pore size was just 2 times the pore size of the primary wick instead of the required 6-10 times. A flight unit with a properly sized CLFR wick will operate entirely successfully.

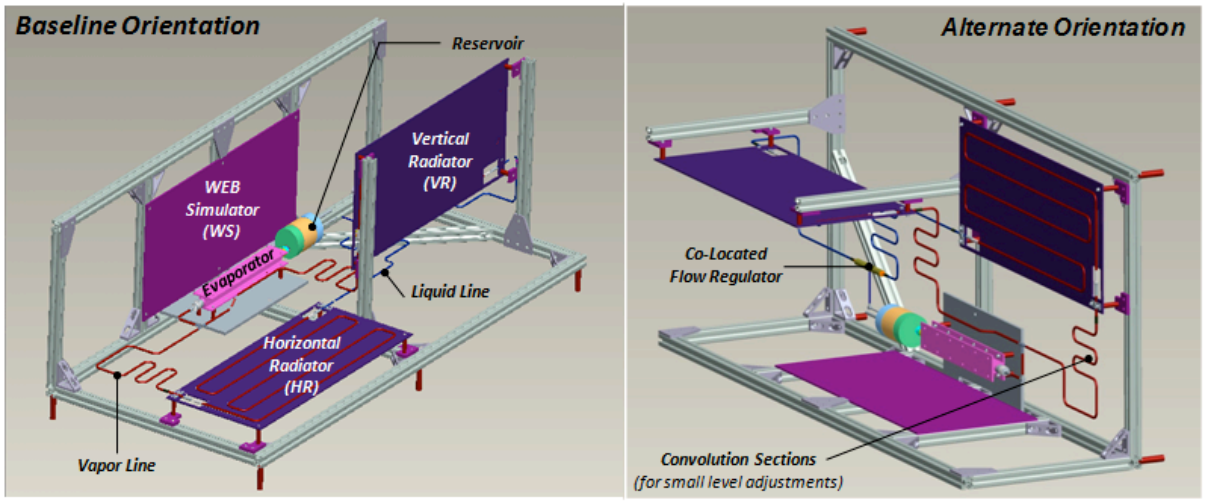

Figure 4. LHP Test System

B. VCHP Stand-Alone Test Unit

The second step in the risk reduction sequence described above was the design and testing of a stand-alone ammonia VCHP that could be integrated into the LHP test system. To simplify integration, the VCHP evaporator, adiabatic, and condenser sections were each limited to 0.2 m in length, which yielded an effective VCHP length of 0.4 m. Thus, the required transport capacity of the VCHP test unit (in order to transport 120 W) was 48W-m. The evaporator and condenser sections were soldered to aluminum saddles with 0.05 m wide mounting interfaces. The adiabatic section was bent (into a U-shape) so that the VCHP evaporator could mount to the WEB simulator plate and the VCHP condenser could mount to the LHP evaporator. To reduce manufacturing cost, the VCHP reservoir was formed by extending the 0.016 m (outer diameter) stainless steel tube 0.3 m beyond the end of the condenser. The reservoir and NCG charge were sized so that the VCHP would provide: (a) fully ON operation with a 321 K evaporator, 315 K condenser, and 288 K reservoir; and (b) fully OFF operation with a 273 K evaporator, 253 K condenser, and 253 K reservoir. The VCHP wick utilized a wire mesh of about 100 microns in pore size with 77% porosity. Additional VCHP features were implemented to improve evaporation and condensation heat transfer performance and provide wetted reservoir operation. Figure 5 illustrates the VCHP stand-alone test unit as it would look (from below) after integration to the WEB simulator plate and LHP evaporator. Ambient lab testing of the stand-alone VCHP yielded operational performance in line with analytical G_{ON} and G_{OFF} predictions.

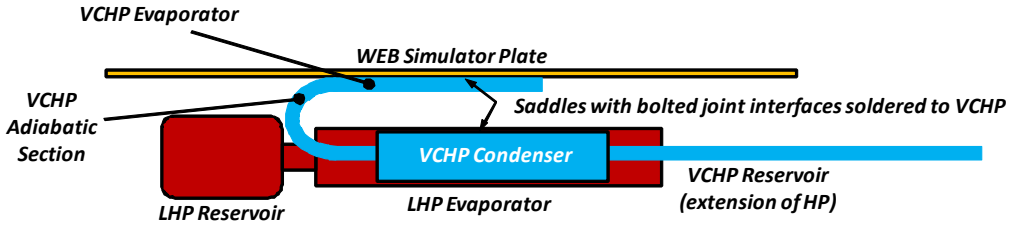

Figure 5. VCHP Stand-Alone Test Unit: ***Shown with WEB Simulator Plate and LHP – Bottom View***

C. VCHP-LHP Test System

The third step in the risk reduction sequence described above was the integration of the VCHP into the LHP test system and the subsequent testing of the VCHP-LHP test system. As notionally depicted in Figure 5, the VCHP condenser flange was bolted to the LHP evaporator flange with Grafoil interface material and the VCHP evaporator flange was bolted to the (0.63 m x 0.25 m) WEB simulator plate with Grafoil interface material. Figure 6 illustrates the VCHP, LHP, and WEB simulator plate prior to their MLI blanketing. Before testing, MLI blankets were placed around the LHP evaporator/reservoir, VCHP adiabatic section, and WEB simulator plate. The VCHP reservoir was left unblanketed for cold-biasing in the hot case.

Figure 7 depicts the key features of the VCHP-LHP test setup.

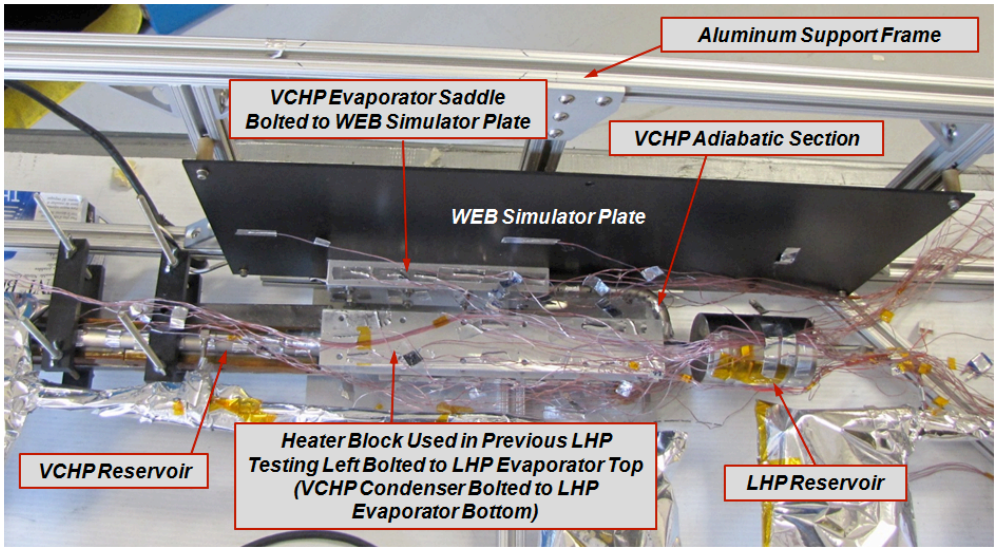

Figure 6. VCHP-LHP Test System: ***VCHP, LHP, and WEB Simulator Plate – Top View***

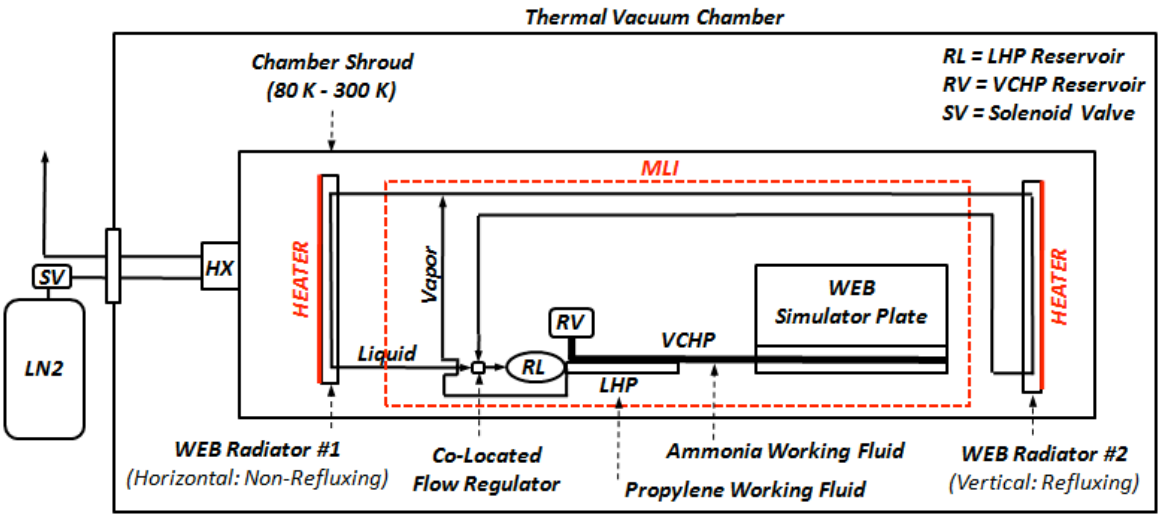

Figure 7. VCHP-LHP Test System: ***Block Diagram of Key Test Setup Elements***

V. Testing

The VCHP-LHP test system was first run on the laboratory bench in an ambient environment to verify system functionality. Following successful laboratory bench testing, the system was inserted into ATK Beltsville vacuum chamber "E", which contains a full 360º LN_2-cooled shroud. The test plan was to conduct a series of tests to evaluate the viability of the VCHP-LHP as the thermal control system for ILN anchor node lunar landers.

A total of 20 tests were conducted by varying heater power to the WEB simulator plate (between 0 and 120 W) with the shroud temperature set to simulate: (i) lunar day (269 K; "hot case"); (ii) 6-day cruise (168 K; "medium case"); or (iii) lunar night (100 K; "cold case"). Tests were conducted with: (a) both radiators active; (b) horizontal radiator (HR) active and vertical radiator (VR) inactive; or (c) both radiators inactive. A radiator was deactivated by applying 100 W of heater power over its surface to suppress condensation. Just one test was conducted with both radiators inactive to determine the effective emittance of the WEB simulator plate MLI. Each test had up to 6 steady-state heater power points. The test procedure involved: (a) setting the sink temperature; (b) applying the WEB simulator plate heater power; (c) waiting for steady-state; and (d) recording the results. Tests were carried out with small adverse tilts on the VCHP and LHP. Table 2 lists the characteristics and measurement goals for the tests.

Table 2. VCHP-LHP Test Matrix

Test #	Case	Date	Start	End	Radiators	Sink (K)	Q (W) Sequence	Measurement Goal
1	Hot	8/21/12	8:51	15:22	Both	269	0, 60, 80, 91	G_{ON}
2	Hot	8/21/12	15:22	21:55	Both	269	0, 60	G_{ON}
3	Cold	8/21-22/12	21:55	13:21	Both	100	3	G_{OFF}
4	Hot	8/22/12	13:21	17:41	Both	269	3, 60	G_{ON}
5	Cold	8/22-23/12	17:41	15:32	Both	100	3	G_{OFF}
6	Hot	8/23/12	15:32	22:33	Both	269	3, 30	G_{ON}
7	Cold	8/23-24/12	22:33	8:08	Both	100	60	G_{ON}
8	Hot	8/24/12	8:08	14:18	Both	269	60, 90	G_{ON}
9	Hot	8/27/12	8:48	15:18	Both	269	3, 60, 80, 0	G_{ON}
10	Hot	8/27/12	15:18	19:27	Both	269	0, 80	G_{ON}
11	Hot	8/27-28/12	18:27	8:04	Both	269	80, 0	G_{ON}
12	Hot	8/28/12	8:04	16:23	Both → HR	269	0, 20, 0, 20, 50, 3	G_{ON}
13	Cold	8/28-29/12	16:23	8:33	HR	100	3	G_{OFF}
14	Cold	8/29/12	8:33	13:45	HR	100	3, 50	G_{OFF} then G_{ON}
15	Med.	8/29/12	13:45	17:21	HR	168	50, 0	G_{ON}
16	Med.	8/29/12	17:21	20:55	HR → Both	168	0, 80	G_{ON}
17	Med.	8/29-30/12	20:55	16:42	Both	168	80, 100, 3, 0, 100	G_{ON}
18	Med.	8/30/12	16:42	21:18	Both	200 → 269	100, 120	G_{ON}
19	MLI	8/30/12	21:18	23:28	None	269	3 (control to 333 K)	ε*
20	Hot	8/30-31/12	23:28	13:24	Both	269 → 273	60, 3, 0	G_{ON}

VI. Analysis

As mentioned, future lunar landers engaged in extended duration science missions will require advanced thermal control hardware that provides autonomous startup and high conductance during the lunar day and autonomous (low control power) turndown with low conductance during the lunar night. To assess the ability of the VCHP-LHP architecture to provide the required performance, both qualitative and quantitative analyses were carried out. Qualitatively, the measured data indicated: (a) autonomous system startup in all environments; (b) stable ON performance in all environments; and (c) effective system shutdown and thermal isolation (OFF performance) in cold environments. This successful performance was the case for both the VCHP-LHP testing described herein and previous stand-alone LHP testing. Quantitatively, total system (WEB-to-radiator) ON and OFF conductance values were computed as were intra-system ON conductance values (WEB-to-VCHP evaporator, VCHP evaporator-to-VCHP adiabatic, VCHP adiabatic-to-VCHP condenser, VCHP condenser-to-LHP evaporator, and LHP evaporator-to-radiator). This section of the paper will focus on the quantitative analyses that were carried out.

A. VCHP-LHP Performance: *ON Conductance*

The total ON conductance is defined as the WEB simulator plate heater power (Q) divided by the total temperature difference (ΔT) between the WEB simulator plate and the active radiators. This ΔT can be broken down into 6 intra-system terms as listed in the leftmost column of Table 3. Also provided in the table are the average ON conductance measurements for all G_{ON} test runs and their corresponding pretest predictions. The pretest predictions were generated in accordance with methods utilized in the previous analytical study[1] (G = W L h). Overall, the measurements are in rough agreement with pretest predictions except for terms 3-4, which together cause the measured total ON conductance to be about a third of the predicted value. However, the primary discrepant term by far is term 3 (the VCHP adiabatic-to-condenser conductance), which is almost an order of magnitude lower than the predicted value. ***To investigate the cause of this discrepancy, an analysis is presented later in this section.***

Table 3. ON Conductance Results: ***Measured Average Values vs. Pretest Predictions***

Intra-System Heat Flow Path	W (m)	L (m)	h (W/m^2K)	G_{PRED} (W/K)	G_{MEAS} (W/K)
1. WEB-to-VCHP evaporator	0.050	0.20	5000 (grafoil)	50	75
2. VCHP evaporator-to-VCHP adiabatic	0.016	0.20	6250 (NH_3 evap.)	20	17
3. VCHP adiabatic-to-VCHP condenser	0.016	0.20	8750 (NH_3 cond.)	28	3.2
4. VCHP condenser-to-LHP evaporator	0.050	0.20	5000 (grafoil)	50	21
5. LHP evaporator-to-LHP vapor	0.016*π/2	0.30	10000 (C_3H_6 evap.)	76	86*
6. LHP vapor-to-LHP condenser	0.005*π/2	4	2000 (C_3H_6 cond.)	64	86*
TOTAL				**6.5**	**2.2**

***43 W/K was measured for paths 5-6 together** (two couplings of 86 W/K in series equals 43 W/K)

While the results indicated in Table 3 were averaged over all G_{ON} cases for simplicity, VCHP-LHP ON conductance was found to autonomously increase with heat load (Q) and decrease with sink temperature (T_S). At a hot sink temperature of 269 K, conductance (in units of W/K) is roughly equal to 0.033 times Q (in units of W). At a medium sink temperature of 168 K, conductance is roughly equal to 0.022 times Q. At a cold sink temperature of 100 K, conductance is roughly equal to 0.015 times Q. A rough generalized formula for the measured VCHP-LHP ON conductance is $G_{ON} = 0.033\ (T_S/269)^{0.8}$ Q. This formula reproduces the test data with a maximum error of about 30% and a mean error of about 10%. Due to the relatively short VCHP evaporator, relatively short VCHP condenser, low cost VCHP reservoir build approach (wherein the VCHP reservoir volume was formed by extending the VCHP tube body), and excessive NCG charge sensitivity due to the small VCHP reservoir volume (see the analysis presented later), the VCHP-LHP ON conductance that will be achievable in a flight unit may be several times higher than the measured value in Table 3 (for a single VCHP-LHP system similar to that shown in Figure 3).

B. VCHP-LHP Performance: *OFF Conductance*

The system OFF conductance is defined as the ***net*** WEB simulator plate heater power (applied heater power less the heat radiated and conducted away) divided by the total temperature difference (ΔT) between the WEB simulator plate and the active radiators. It was assumed that all the heat lost by the WEB plate was via radiation through the MLI blanket. The effective MLI emittance ε^* was found to be 0.016 (by analyzing Test 19 steady-state results). Given a WEB simulator plate two-sided area of 0.32 m^2, the heat lost radiatively by a 273 K WEB simulator plate to a 100 K sink is 1.6 W. Table 4 lists the calculated OFF conductance values for the three runs where the system attained a steady-state with a 100 K shroud. The small negative ΔT values in Table 4 represent thermocouple inaccuracy and indicate that the VCHP evaporator and WEB simulator plate are essentially at the same temperature. The predicted system OFF conductance with a shutdown LHP and blocked VCHP is 0.00028 W/K. This predicted

value is comprised of a predicted LHP OFF conductance of 0.0003 W/K (conduction in the vapor/liquid transport lines) in series with a predicted VCHP OFF conductance of 0.006 W/K (conduction in the adiabatic wall, wick, and liquid ammonia). The data provided in Table 4 indicate average values for the measured LHP and VCHP OFF conductance of 0.04 W/K (see G4) and 0.016 W/K (see G2), respectively, yielding a total measured system OFF conductance of 0.01 W/K. Additional details relating to the measured and predicted OFF conductance behavior of the system is provided in the next subsection. The focus of that discussion is on the LHP, because the greatest OFF conductance system improvement can be attained if the LHP can attain its predicted level of OFF performance.

Table 4. OFF Conductance Results: *Intra-System and Total System Performance*

				WEB - VCHP/E		VCHP/E - VCHP/C		VCHP/C - LHP/E		LHP/E - Radiator		LHP-VCHP System	
Test	QWEB (W)	QLOSS (W)	Time of SS	ΔT1 (K)	G1 (W/K)	ΔT2 (K)	G2 (W/K)	ΔT3 (K)	G3 (W/K)	ΔT4 (K)	G4 (W/K)	ΔTTOT (K)	GOFF (W/K)
3	3	1.6	8:18	-0.38	-4.00	94.05	0.016	0.745	2.01	30.56	0.050	124.98	0.0112
5	3	1.6	15:22	0.13	10.91	108.98	0.014	0.286	5.35	38.28	0.039	147.68	0.0095
13	3	1.6	8:30	-0.34	-4.44	81.61	0.018	0.029	52.5	56.20	0.027	137.50	0.0100

C. LHP Shutdown Behavior

If ideal LHP and VCHP shutdown behavior were attained between hot/cold limits of 273 K/100 K, total heat loss through the system would be just 0.048 W. LHP evaporator cooling would cease at a temperature of 261 K, which is the LHP hot-side/VCHP cold-side temperature where VCHP and LHP OFF heat flows are equal . Two cases of LHP shutdown were investigated: (1) shutdown with both radiators active; and (2) shutdown with just the HR active. Figure 8 illustrates the results of Test 5 (shutdown with both radiators active) and Figure 9 illustrates the results of Test 13 (shutdown with HR active). In Figure 8, LHP evaporator cooling appears to have slowed a temperature of 165 K (-108 ºC), possibly due to propylene viscosity effects. In Figure 9, LHP evaporator cooling appears to have slowed at a temperature of 200 K (-73 ºC), possibly due to autonomous shutdown. The difference between the two cases suggests that a non-refluxing system will exhibit slightly better LHP evaporator shutdown behavior than a refluxing system, though neither is likely to achieve ideal performance autonomously. Additional testing is needed with control power induced LHP shutdowns at higher temperature (where heater power is used to raise the LHP reservoir temperature above the LHP evaporator temperature) to examine whether ideal LHP shutdown behavior is attainable with a small burst of control power or whether steady control power is necessary. Of course, even with non-ideal LHP shutdown performance, the measured switching ratio of 220 (or the modestly higher switching ratio attainable with proper NCG charging as discussed in the next subsection) may be sufficient for lunar lander variable heat rejection. NASA/MSFC has the VCHP-LHP test hardware and additional testing is planned for the near future.

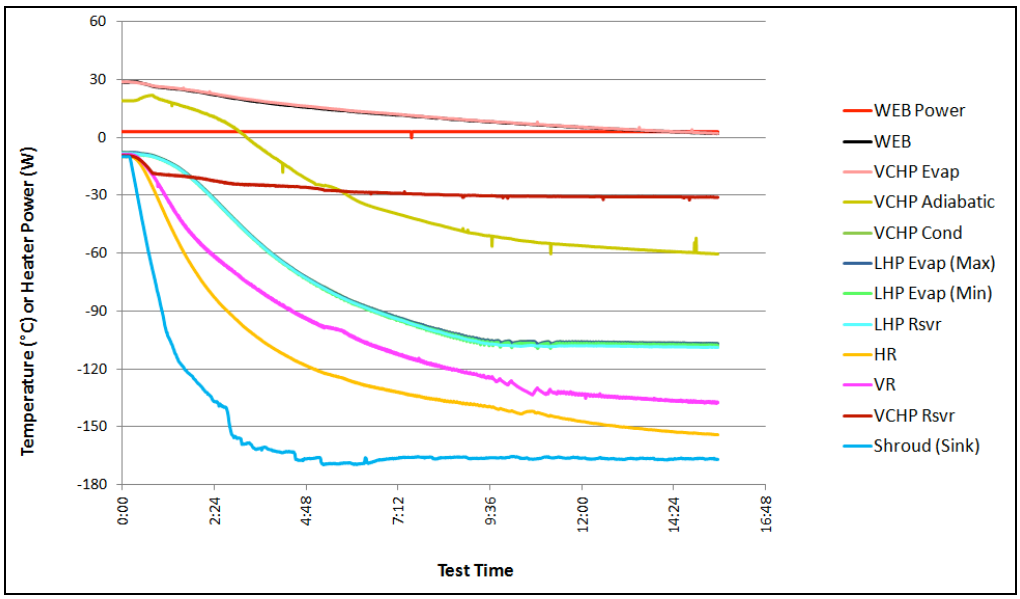

Figure 8. LHP Shutdown Behavior with HR Active and VR Active (Test 5)

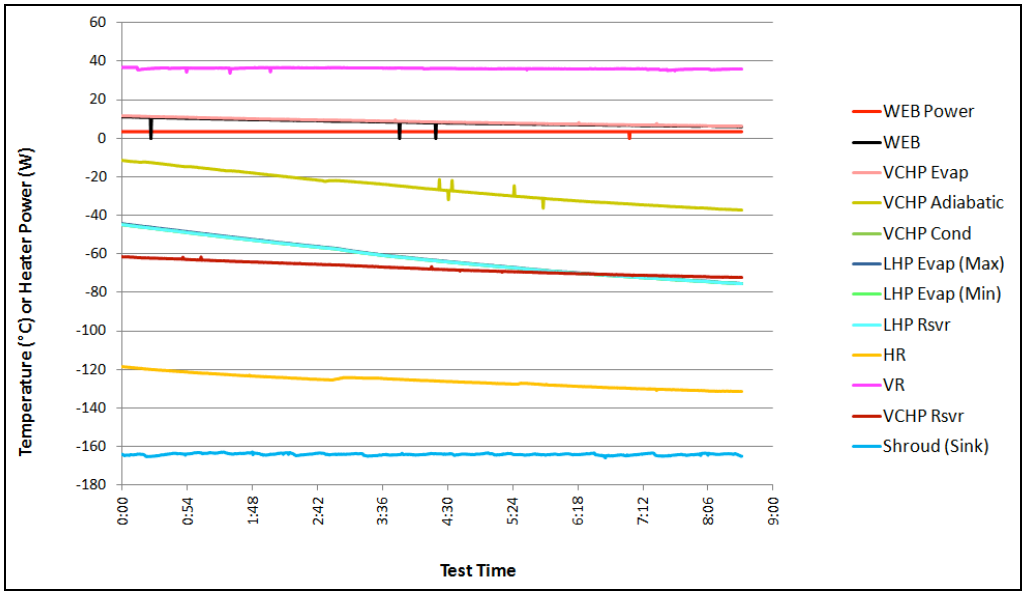

Figure 9. LHP Shutdown Behavior with HR Active and VR Inactive (Test 13)

D. VCHP Condensation Conductance

The measured system ON conductance of 2.2 W/K is just one-third of the predicted system ON conductance. The source of this discrepancy is the VCHP condensation conductance. One hypothesized cause is excess NCG blockage of the condenser. To examine this hypothesis, a detailed analysis was carried out to predict the NCG front location based on the NCG charge and measured system temperatures. A plot of condenser open percentage vs. measured VCHP condensation ON conductance was prepared for each steady-state (G_{ON}) power point. The results illustrated in Figure 10 suggest that ON conductance testing was carried out with a VCHP condenser that was (on average) 60-70% blocked. Thus, the VCHP ON conductance was lower than it would have been had the condenser been fully open. Figure 10 predicts a fully open VCHP condenser would have had a conductance of 8.3 W/K (instead of just 3.2 W/K), which would have increased the measured system ON conductance to 3.8 W/K. It is likely that the VCHP used in this test system, because of its small reservoir, is too sensitive to NCG charge. It is also likely that a future flight VCHP with a larger reservoir would be much less sensitive to NCG charge. The design of the VCHP condenser should also be investigated, as this analysis only explains a portion of the discrepancy.

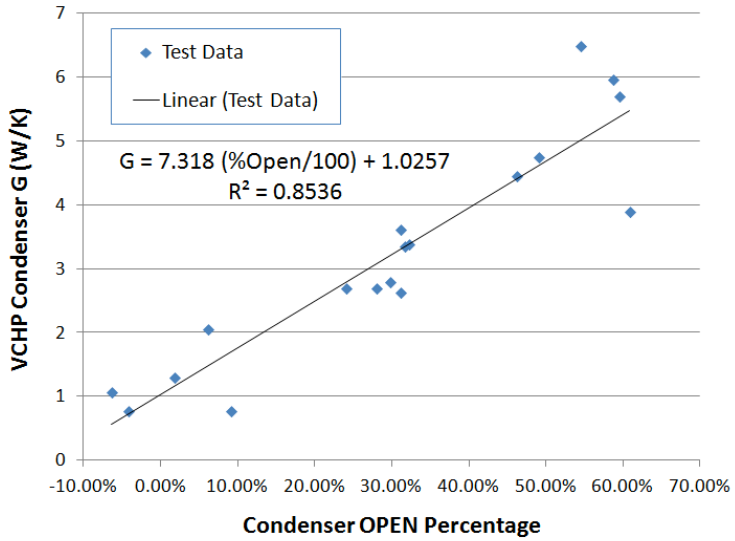

Figure 10. VCHP Condenser Open Percentage During ON Conductance Testing

E. VCHP Freeze-Tolerance

By virtue of the wire mesh wick that extends from the VCHP evaporator to condenser and the small charge of noncondensable gas (NCG), VCHPs are intrinsically freeze-tolerant. The physics underpinning VCHP freeze tolerance is depicted graphically in Figure 11. Essentially, as the VCHP condenser nears the working fluid freezing point (T_{MELT}), NCG forces liquid to freeze within VCHP wick structures. Thus, melting can take place benignly without putting stress on the VCHP wall. In a few of the tests described herein including Test 5, which is illustrated in Figure 8, the VCHP condenser was frozen then thawed a few times with no adverse effects. Additionally, any VCHP flight unit should be designed with a reservoir that is also freeze-tolerant. A freeze-tolerant VCHP reservoir will probably require the primary VCHP wick to extend its entire length and it may also require specialized internal wicking to prevent liquid from freezing as a slug that could later melt and apply undue force to the reservoir wall.

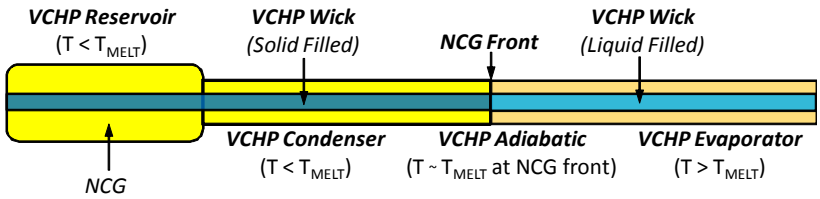

Figure 11. VCHP Wick and NCG Provides Intrinsic Freeze-Tolerance

VII. Future

Future implementations of VCHP-LHP technology are envisioned to be capable of meeting variable heat rejection (VHR) mission requirements such as those specified in a recent NASA NRA[2]. The requirements specified in this NASA document describe a 3-phase mission with: (1) a low Earth orbit (LEO) phase with 1.2 kW heat rejection, 180-200 K sink, and 100 hour duration; (2) a trans-planetary coast (TPC) phase with 1 kW heat rejection, 70 K sink, and 100 hour duration; and (3) a planetary surface operations (PSO) phase with 5.8 kW heat rejection, 230 K sink, and 200 hour duration. The VCHP-LHP system described herein is a viable candidate for such a variable heat rejection mission providing it can be effectively scaled up to higher power.

Scaling the VCHP-LHP system tested herein to higher power is postulated to be achievable by simply increasing the number of VCHP and LHP elements like building blocks. For example, if generic capabilities of 188 W per VCHP and 750 W per LHP are assumed, a 6 kW multi-VCHP, multi-LHP system could be constructed with 32 VCHPs and 8 LHPs as notionally illustrated in Figure 12.

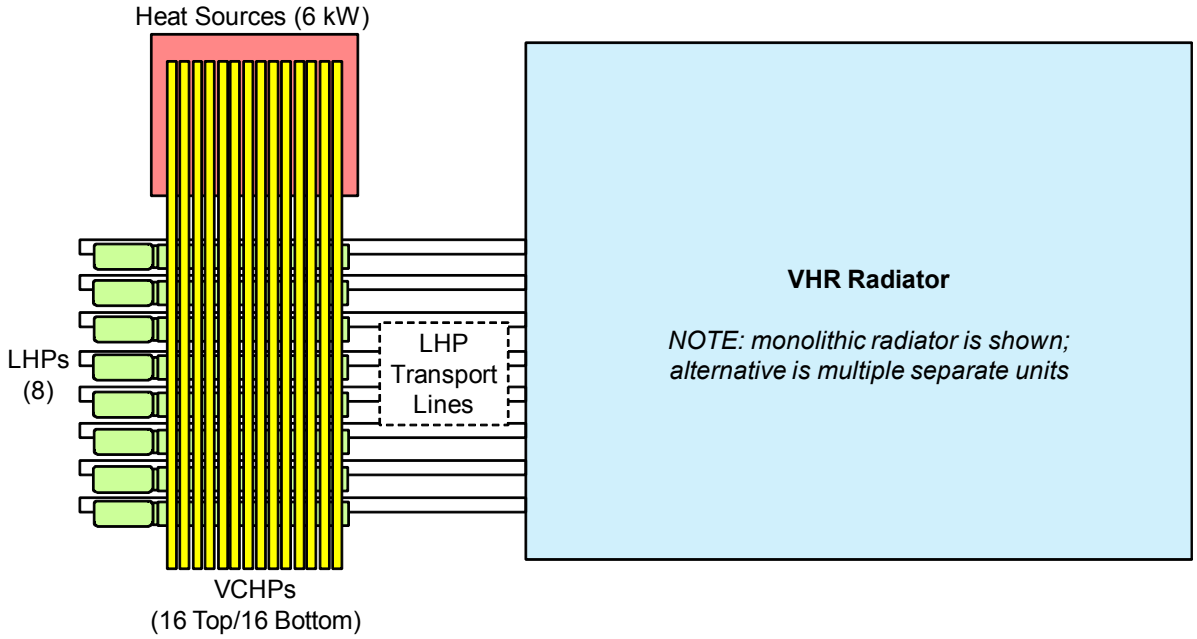

Figure 12. Notional VCHP-LHP High Power Capable Architecture

The technical challenges that are likely to be encountered in scaling the VCHP-LHP architecture to high power include the following: (1) identify system architecture modifications needed for multi-kW missions; (2) investigate the scalability of passive operation (that is, if a low power VCHP-LHP can be made to operate purely passively, can that passivity be maintained at higher power); (3) identify and investigate operational requirements and idiosyncrasies; (4) identify acceptable VCHP-LHP working fluids; and (5) identify system integration requirements and/or limitations. The authors sincerely hope that additional NASA funding will be garnered in the near future to help address the foregoing technical challenges, although some of those challenges are already under investigation.

For example, one technical need that was identified during VCHP-LHP testing was the requirement to provide VCHP reservoir cold-biasing to maximize positive control. It was postulated that the LHP liquid return line could be utilized for that purpose. Figure 13 depicts a possible configuration that utilizes the LHP liquid return line for VCHP cold-biasing. This novel idea may obviate the need leave the reservoir unblanketed as shown in Figure 5. A number of other such novel ideas are currently being evaluated to address future VCHP-LHP technical challenges.

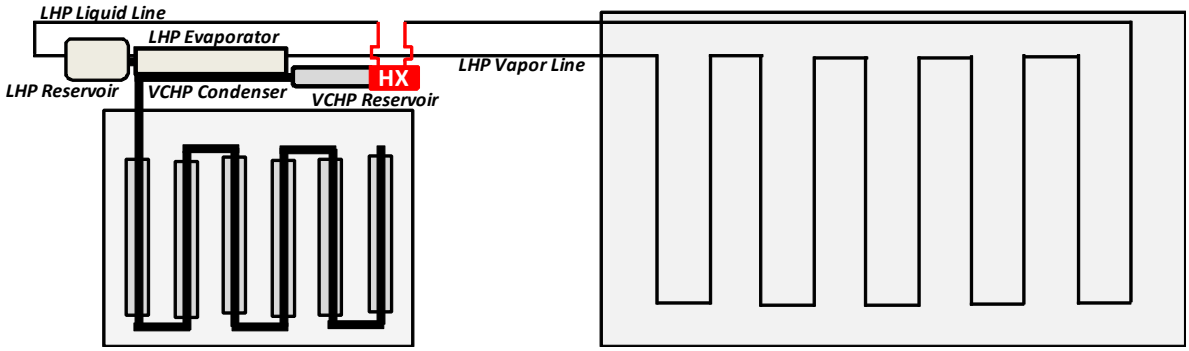

Figure 13. VCHP Reservoir Cold-Biasing with LHP Liquid Return Line

VIII. Conclusion

This study has shown that the VCHP-LHP thermal switching system is a viable candidate for lunar missions, such as the International Lunar Network (ILN) mission, requiring the ability to transport and reject heat efficiently during the hot lunar day, requiring the ability to thermally isolate and conserve heat/power during the lunar night, and requiring the ability to reliably switch between the two modes of operation with minimal resources. When fully implemented, the VCHP-LHP architecture overcomes LHP limitations by utilizing VCHP advantages and overcomes VCHP limitations by using LHP advantages and is ultimately capable of providing thermal switching ratios of 1000 or more (e.g., the potential turn-down ratio of the system tested herein is 21667 using predicted VCHP-LHP ON/OFF conductance values of 6.5 W/K ON conductance and 0.0003 W/K OFF conductance). The VCHP-LHP system tested herein was hampered slightly by design limitations that include a relatively short VCHP evaporator, a relatively short VCHP condenser, and a small VCHP reservoir that made proper NCG charging so problematic that the system operated with a 60-70% (on average) gas-blocked VCHP condenser during system ON conductance testing. Despite these limitations, the VCHP-LHP system started and shut down autonomously and was able to provide ON conductance values between 2-4 W/K, OFF conductance isolation of 0.01 W/K, and switching ratios of 200-400. Overall, the test program was very successful and future work could entail scaling the architecture to higher power for anticipated future NASA applications involving variable heat rejection.

Acknowledgments

The authors would like to thank the NASA Marshall Space Flight center for funding the work reported on herein.

Appendix

The International Lunar Network (ILN) was one of several potential robotic lunar surface science missions for which the VCHP-LHP thermal switching system described in this paper was developed.[3] Figure 14 illustrates a notional ILN solar powered lander concept with a parabolic reflector radiator shown on the side of the lander. For lander locations in the northern hemisphere, the lander would position itself prior to landing so that the radiator would point north after landing. Thus, the radiator will typically point away from the sun. Figure 15 illustrates a

closeup view of the stacked parabolic reflector radiator concept. The radiator blue surfaces represent radiating fins that protrude from a conductive back plane. The radiator gold surfaces represent parabolic reflectors that specularly reflect IR heat from the hot lunar surface away from the radiating fins as well as deflect solar input from the fins, allowing the radiating fins to have a limited but efficient view to cold space, providing a relatively cold 269 K sink during the lunar day. If a VCHP-LHP system were utilized for thermal control on this conceptual ILN lander, a series of LHP condenser lines would be thermally linked in series or parallel to the multiple radiating fins.

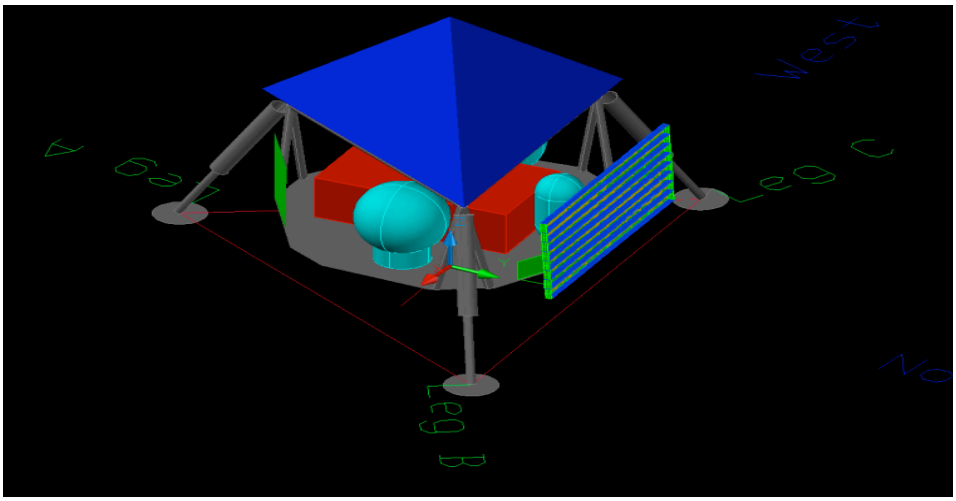

Figure 15. ILN Solar Powered Lander Concept

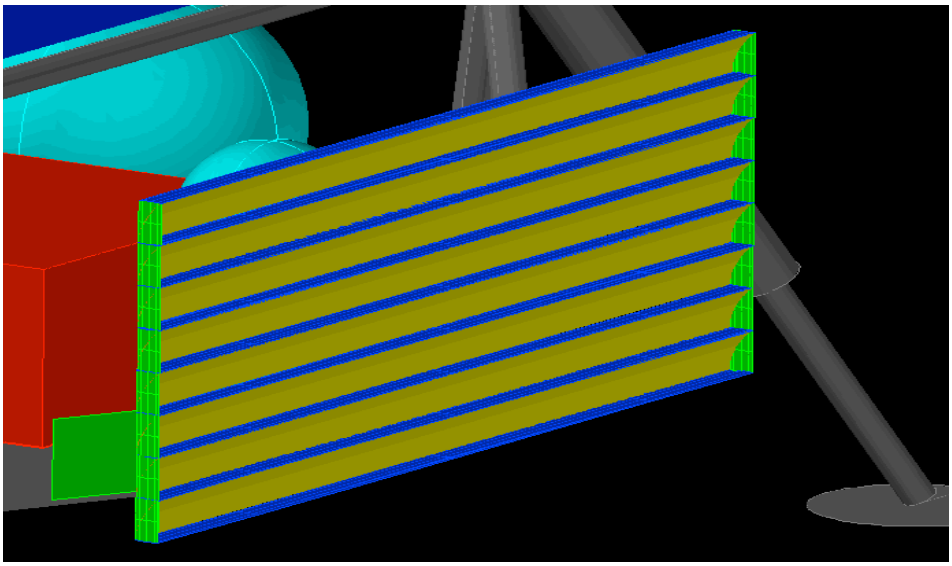

Figure 14. Stacked Parabolic Reflector Radiator Concept

References

[1]Bugby, D. C., Farmer, J. T., O'Connor, B. F., Wirzburger, M. J., Abel, E. D., and Stouffer, C. J., "Two-Phase Thermal Switching System for a Small, Extended Duration Lunar Surface Science Platform," SPESIF Conference, JHU/APL, 2010.

[2]NASA Research Announcement (NRA) NNL12A3001N, Appendix C: Technology Development for Variable Heat Rejection, Issued July 23, 2012.

[3] Farmer, J. T., "Reference on Lunar Lander Missions"